J Biochem Technol (2021) 12(2): 48-61
https://doi.org/10.51847/xEKyD9bMjR
ISSN: 0974-2328

Theoretical Investigation of Some Donepezil-based Derivatives as Dual Inhibitors for beta-Amyloid- and Cholinesterase Enzymes

Assia Meziane, Amina Ghomri, Salim Bouchentouf*, Mohamed El-Shazly

Received: 12 March 2021 / Received in revised form: 01 May 2021, Accepted: 09 May 2021, Published online: 21 June 2021

Abstract

To treat Alzheimer's Disease (AD), which is the most prevalent form of dementia, cholinesterase enzymes (AChE and BuChE) and amyloid-beta (Aβ) are attractive targets. In this work, different computational approach namely Density Functional Theory (DFT), Molecular Docking, and multi-QSAR modeling were performed on 22 donepezil-based derivatives which were reported as potent dual Aβ and (AChE and BuChE) inhibitors. The molecular geometries of the studied derivatives were carried out using GAUSSIAN 09 software with the level of theory (DFT, 6/31g*). The dual inhibitors adopted minimum energy. The results pointed out the importance of the inhibitors' geometries in enzyme inhibition. The QSAR models elaborated by means of Molecular Operating Environment (MOE) package, showed good statistical values for targets AChE (R^2adj = 0.976, q2 = 0.871, RMS = 0.130), BuChE (R^2adj = 0.976, q2 = 0.554, RMS = 0.092) and Aβ **(**R^2adj = 0.861, q2 = 0.525, RMS = 0.113). To identify the binding pattern between the ligands and target enzymes, we implemented molecular docking studies for the datasets. The obtained information was related to the essential structural features that were related to the QSAR of the predicted models.

Keywords: Molecular docking, ButylCholinesterase, Quantitative structures activity relatioships, Acetylcholinesterase, Density functional theory, Donepezil

Assia Meziane, Amina Ghomri
High School of Applied Sciences (ESSA) of Tlemcen, BPN° 165 Belhorizon Tlemcen, Algeria.
Laboratory of Natural and Bioactive Substances (LASNABIO), Chemistry Department, B.P 119, Tlemcen (13000), Algeria.

Salim Bouchentouf*
Department of Process Engineering, Faculty of Technology, Tahar Moulay university, Saida, Algeria.
Laboratory of Natural and Bioactive Substances (LASNABIO), Chemistry Department, B.P 119, Tlemcen (13000), Algeria.

Mohamed El-Shazly
Department of Pharmacognosy, Faculty of Pharmacy, Ain Shams University, Abbassia, Cairo, Egypt.
Department of Pharmaceutical Biology, Faculty of Pharmacy and Biotechnology, The German University in Cairo, Cairo 11835, Egypt.

***E-mail:** bouchentouf.salim@yahoo.fr
salim.bouchentouf@univ-saida.dz

Introduction

The most common type of dementia is Alzheimer's Disease (AD) (Ronson, 2011; Uddin & Amran, 2018). AD affects over 44 million people worldwide. By 2030, the number of patients will be doubled and even tripled by 2050 (Harris, 2019). The worldwide cost of dementia was estimated at 604 billion USD in 2010 and is expected to increase exponentially. To tackle this problem, it is advisable to develop early detection methods and effective therapeutics (Tappen, 1997; Bamidis *et al.*, 2020; Lilford & Hughes, 2020). AD may also affect patients with noncognitive disorders such as depression anxiety, hallucinations, and delusions (Vicente *et al.*, 2015). Although AD pathogenesis is complex and unclear, there are several developed theories, but none of them revealed the specific cause of AD (Hardiman *et al.*, 2016; Lilford & Hughes, 2020). Common targets were identified and explored over the last two decades. The main hallmarks such as amyloid plaques (Lee, 2000; Ronson, 2011), peptide aggregates, the tau protein aggregates (Stonebrook, 2007; Sigurdsson *et al.*, 2012) discovered in AD patient brains were correlated with most of these targets. AD development was affected by the role of cholinergic deficit (Banner & Nixon, 1992; Piguet & Poindron, 2012). Aβ peptides are APP (Amyloid Precursor Protein) proteolytic by-products that consist of 42 (Aβ1−42) amino acids and40 (Aβ1−40). One of the strategies to cure AD is to block the generation of Aβ peptides aggregation. AChE, BuChE, and Aβ aggregation inhibitors emerged as effective tools for AD treatment. It was suggested that the effectiveness of the treatment was significantly improved by the dual inhibition strategy of these enzymes (Lajtha & Banik, 2001; Kuncharoenwirat *et al.*, 2020; Sargazi & Taghian, 2020). The evaluations of *in vitro* Aβ aggregation inhibitors, progress, are time-consuming and labor extensive task. Computer-Aided Drug Design (CADD) (Kapetanovic, 2008) tools including molecular modeling in combination with Quantitative Structure-Activity Relationship (QSAR) (Li *et al.*, 2019; Kasmi *et al.*, 2020; Mahmud *et al.*, 2020) and molecular docking (Roy *et al.*, 2020) are used to evaluate a ligand activity and the kind of interactions into the protein active site (Taha & AlDamen, 2005). They provide useful tools for the design of new drugs to save time and money (Gu *et al.*, 2021).

The biological activity of donepezil as anti-Alzheimer diseases has been the subject of different investigations. Shamsi *et al.* (2020), with human transferrin, applied molecular docking, calorimetric, and spectroscopic insights into the role of donepezil

as an anti-Alzheimer's drug. Aranda-Abreu *et al.* (2011) studied and discussed the absorption of donepezil after oral administration and compared it to tacrine. They found that donepezil was better tolerated by patients and caused fewer adverse reactions. Wallin *et al.* (2007) evaluated the results of three-year donepezil treatment and from their observation, the obtained results indicated a positive outcome in the routine clinical setting. To shed more light on donepezil derivatives as anti-Alzheimer's drugs, we selected 22 derivatives **(Table 1 and Figure 1)** (Khosravan *et al.*, 2017) and evaluated their cholinesterase enzymes (AChE and BuChE) inhibitory activity and amyloid-beta (Aβ) in silico (Yerdelen *et al.*, 2015).

Materials and Methods

Dataset and Target Preparation

The molecular optimized geometries of the 22 donepezil derivatives were optimized using the DFT/ B3LYP (Daramola *et al.*, 2010). Functional hybrid, with the 6-31g* basis set was implemented in the Gaussian 09 software (Hiscocks & Frisch, 2009), the stability of geometries was checked by the absence of the imaginary frequencies. The ligands properties **(Table 1)** were obtained by MOE software (Höltje, 2008; Kukol, 2008; Royal Society of Chemistry (Great Britain), 2014) results showed that the studied ligands were nontoxic, and the molecular weights were less than 500. The toxicity was done by MOE software.

The X-ray crystal structures of the targets, AChE (PDB ID: 1HBJ), BuChE (PDB ID: 4BDS), and Aβ (2BEG) were downloaded from the RCSB Database (http://www.rcsb.org/pdb). These three PDBs were chosen for modeling research since their crystal structures are in a condition that shows the pharmacological target for developing new drugs to treat AD.

QSAR Modeling and Models Validations

Biological Activities

Acetylcholinesterase (AChE), butyrylcholinesterase (BuChE), and Amyloid-beta (Aβ) inhibitory activities of a series of 22 donepezil-like amide secondary derivatives were taken from Kadir *et al.*'s work (Yerdelen *et al.*, 2015), each activity was mentioned as IC_{50}(μM) for (AChE) and (BuChE), and as a percentage for Aβ inhibitory activity. Values were expressed as mean ± standard error of the mean of three independent experiments. Values were converted to pIC_{50} as $pIC_{50} = -\log IC_{50}$. The dataset was divided into a training set containing 17 compounds and a test set composed of 5 compounds **(Table 1)**.

Molecular Descriptors Generation

Molecular descriptors were generated using MOE programs to predict the correlation between these parameters and their activities by developing a linear model (Partial Least Squares regression (PLS) (Wehrens & Mevik, 2007; Kovačević *et al.*, 2018). In this work, 12 QSAR models were developed **(Tables 2)** using the experimental IC_{50} data. Calculations were done using a total of 365 different descriptors exploited in the MOE software. These sets of descriptors were first pre-processed with a variance threshold of 0.0001 and passed through a correlation coefficient of 0.99 to eliminate correlations between the input descriptors and noise level. A Genetic Algorithm (GA) was applied to select the best possible set of descriptors for QSAR modeling from the pre-processed pool of descriptors. This "descriptor elucidation" procedure allowed us to select the four most significant descriptors to build our QSAR models which were: AChE (chi0v_C, PEOE_VSA_POL, vsurf_D5, vsurf_Wp4), Bthe (npr1, vsurf_CP, vsurf_CW4, vsurf_Wp6) and for Aβ (a_ICM, density, vsurf_HL1, vsurf_ID1). The identified descriptors were the most pertinent for our elucidation as they reflect the required activities of all the studied molecules, assuming that a change of the molecular structure modifies the inhibitory activity of donepezil derivatives.

Regression Analysis

Data fitting was accomplished using PLS regression analysis. When there are many independent variables in the trial descriptor pool relative to the number of the dependent variables, the pIC_{50} endpoints, this data fitting technique becomes useful. When there is no method for ranking the individual members (molecular descriptors) of the trial descriptor pool and/or knowing possible inter-relationships among the training set of descriptors, the PLS is applied. Regression analysis was done by PLS method, because of the largest of the independent variables in the trial descriptor compared with the number of dependent variables, pIC_{50}, our choice is justified because PLS is the best one as there is no method for ranking the individual members (descriptors) or distinguishing the inter-relationships between those descriptors. The PLS regression was used to build a single QSAR model that contains the entire trial descriptor pool. Both R^2 and the leave-one-out (LOO) cross-validated correlation coefficient, q^2, were employed to characterize the quality of the resultant QSAR models.

Molecular Docking Procedure

Using MOE, molecular docking studies were done aiming to find the best conformation of the donepezil derivatives in protein binding sites. The downloaded 3D structures of the protein complexes were protonated, and energy minimized in an MMFF94x force field to a gradient of 0.0001 kcal/mol/Å (Engh & Huber, 1991). Using the MOE-Alpha Site finder, the active sites were generated. The dummy atoms were created from the obtained alpha spheres. Prepared protein structures are presented in **Figure 2** for AChE, Bthe and Aβ prepared enzymes and the active sites are also presented. The 3D structures of all compounds were built by GaussView06, structures were optimized and saved as Mol Folders. Using the MOE program, the database set was created, and this database was used as input MOE-docking. We used the default settings of the parameters with Ligand Placement (Triangle Matcher) and Rescoring (London dG) implemented in the MOE program (Chemical Computing Group Inc, 2016). Furthermore, the LigX feature of MOE was used to find the hydrogen bonding interactions

between the ligand and receptor protein. The best docking scores were used for the calculation of binding energy.

Results and Discussion

DFT Calculations and QSAR Modeling

To build the QSAR models, molecular geometries were optimized using the B3LYP/6-31g* and the database was created. The elaborated QSAR models (Tables) revealing the correlations between the AChE, BChE, and Aβ inhibitory activities, and the corresponding equations are also presented in the above tables.

The terms were defined including $N_{Training}$ the number of molecules in the training set, N_{Test} the number of molecules in the test set, R^2_{CV} (Q^2) the LOO cross-validated coefficient, RMSE the root mean square error, and R^2 the correlation coefficient. The absolute difference between the activity field and the value of the model is $Z-SCORE, which is divided by the square root of the mean square error of the data set. For the external validation, the values of R^2_{test} (correlation coefficient), RMSE test (Root Mean Square Error) were selected corresponding to the best models for each enzyme.

R^2 allowed us to compare the experimental and predicted studied activities, which is the protein inhibition. A good model must have a value of R^2 above or equal to 0.5 whereas RMSE is mostly used to decide if the QSAR model possesses the predictive quality reflected in R^2. It showed the error between the mean of the experimental values and the predicted properties. If RMSE is above 1 (RMSE >1), the model has a poor ability to foretell the properties even with a good R^2 value. However, R^2 and RMSE parameters are not sufficient to judge the QSAR validity, that is why cross-validation is required. Cross-validation R^2cv is used to allow the determination of how large the model can be used for a random data set and to evaluate the predictive power of the model's equation. On the other hand, the standardized value, which specifies the exact location of an X value within a distribution by describing its distance from the mean in terms of the standard deviation units is represented by XZSCORE and ZSCORE. This subset must be examined carefully to detect errors or to determine new descriptors to be calculated. ZSCORE must be less than 2.5 to suggest that the QSAR model is good to be used. Internal validation is not sufficient to estimate the predictive power of a QSAR mode.l. Golbraikh and Tropsha suggested (Golbraikh *et al.*, 2003) the following statistical characteristics of the test set: correlation coefficient *R* between the predicted and observed activities, coefficients of determination (R^2_{test}) the correlation between the predicted and the experimental inhibition activities are represented in **Figure 3** for AChE, BuChE, and Aβ respectively. They consider a QSAR valid model with $R^2_{test} > 0.6$ taken as an indicator of good external predictability.

To highlight the validity of our models for each enzyme as well as the chosen descriptors contributions on each activity, we calculated the statistical parameters shown in **(Tables 2 and Figures 3)** for the internal validation and correlation coefficients for the external validation **(Figure 3)**.

In the case of AChE, **Table 1** and **Figure 3** showed that among the four elaborated models, model number 2 demonstrated the best results with the value $R^2 = 0.88$ and RMSE = 0.13. For the cross-validation and $R^2_{CV} = 0.58$ with $Z-SCORE less than 2.5 ($0.6946 < ZS < 1.142$), our results allowed us to confirm the correlation between the six selected descriptors (E_str; PM3_IP; PM3_LUMO; SMR_VSA2; SMR_VSA3; vsurf_Wp4) and the donepezil derivatives. AChE inhibition specified as IC_{50} correlation plot between the predicted and experimental activities for AChE enzyme confirmed that model 2 is the best. Since the internal validation is insufficient to judge the model validity, we proceeded to an external validation using five molecules from the dataset which were not used in the model elaboration. **Figure 3** gave the values and correlations between the experimental and theoretical activities obtained for the five test molecules. Our results showed that the selected model 2 can be used to predict the donepezil derivatives activities. The residual values between our predicted values and the experimental ones varied from 0.0013 to 0.1189. Those values are considered excellent values for the prediction of inhibitory activities. As indicated by Jalali-Heravi and Kyani, we noted that the positive and negative values varying the residuals on both sides of zero showed that there was no systemic error (Jalali-Heravi & Kyani, 2004). To predict the pAChE inhibitory activities, this model can be applied successfully. The correlation coefficient between the predicted and experimental values is $R^2 = 0.96$ and this value was also considered excellent.

The selected descriptors chosen in the best model 2 suggested that E_str, PM3_LUMO, and vsurf_Wp4 were associated with a negative coefficient, indicating that increasing the value of these descriptors was unfavorable to the acetylcholinesterase inhibitory activity for each molecule PM3_IP, SMR_VSA2, and SMR_VSA3 descriptors that were associated with a positive coefficient suggesting that the inhibitory activity of the molecules increased with the increase of the approximate accessible van der Waals surface area of the molecule. The same conclusions could be made for the ionization potential of donepezil derivatives.

In case of BuChE, **Table 2** and plot 2 showed that among the four elaborated models, model number 6 is best model showing the best results with values of $R^2 = 0.74$, RMSE = 0.09 and the cross-validation correlation coefficient $R^2_{CV} = 0.55$ with $Z-SCORE less than 2.5 ($0.52 < ZS < 0.71$). Between the six selected descriptors. E_oop, MNDO_dipole, vsurf_DD12, and the vsurf_ID4 were associated with negative coefficients, so an increase in these quantities decreased the inhibitory activities. The increase of the vsurf_HB3 and vsurf_ID3 corresponded to an increase of the inhibitory activity. These descriptors are useful in pharmacokinetic property prediction. The correlation plot between the predicted and experimental activities for the BuChE enzyme is presented in **Figure 3** and it confirms that model 6 is the best one between the four established models. For the external validation, we used five molecules from the dataset which were not used in the model elaboration. **Table 2** and plot 2 provided

the values and correlations between the experimental and theoretical activities obtained for the five tested molecules. Our outcomes revealed that the selected model 6 can be used to predict the donepezil derivatives inhibitory activities. The residual value between our predicted values and the experimental ones varied from 0.039 to 0.06. These values are also considered excellent values for the prediction of BuChE inhibitory activity. The correlation coefficient between the predicted and experimental values (plot) was R^2_{test} = 0.95, which was also classified as an excellent value.

In the case of Aβ, **Table 2** and **Figure 3** showed that among the four elaborated models, model number 11 is the best model with R2 = 0.76 and RMSE = 0.11. For the cross-validation and R^2CV = 0.52 with $Z-SCORE less than 2.5 (0.01 < ZS < 2.3), our results allowed us to confirm the good correlation between the six selected descriptors (a_ICM; density; vsurf_HL1; vsurf_ID1; vsurf_ID2) and the Aβ inhibition by donepezil derivatives specified as IC_{50}. All parameters were expressed with positive coefficients, suggesting that an increase in the values of these descriptors will lead to an increase in the inhibitory activity. The correlation plot between the predicted and experimental activities for the Aβ enzyme is presented in **Figure 3** and it confirms that model 11 is the best. We also proceeded to an external validation using five molecules from the dataset which were not used in the model development. **Table 2** and **Figure 3** provided the values and correlations between the experimental and theoretical activities obtained for the five test molecules. Our results suggested that the selected model 11 can be used to predict the donepezil derivatives activities. The predicted values were very close to the experimental values and they were considered excellent values. The correlation coefficient between the predicted and experimental values **(Figure 3)** was R^2 = 0.90, which was also considered an excellent value.

Molecular Docking Simulation

To prepare the enzymes, we identified the active site residues of both cholinergic and amyloid-beta targets, the active-site residues in AChE **(Figures 4)** are GLY118, GLY119, and ALA 201, which create the catalytic triad. The active-site residues for BuChE **(Figures 4)**: HIS438, SER198, and GLU325. For the Aβ **(Figures 4)** the active site did not show the potent residues because the downloaded structure was not complexed with any reference ligand. All the prepared enzyme structures and the fixed sites are presented in **Figures 4**.

Studies on molecular docking proceeded with the 22 molecules database designed by MOE. The AChE, BuChE, and Aβ protein-ligand complexes were evaluated by estimating various types of interactions (non-polar and polar such as H-bonding interactions, electrostatic interactions, van der Waal's interactions, hydrophobic interactions for ligands). The results indicated that the lowest docking score AChE (-8.1299 kcal/mol, ligand 4), BuChE (-7.0399 kcal/mol, ligand 14), and Aβ (-4.8651 kcal/mol, ligand 15) were the best docking score and other scores were calcified respecting this order (that all scores were calcified and the lowest founded for each enzyme was the one given). **Figure 4** showed the 2D Protein-ligand interaction maps for the 22 molecules. The figure showed that the best dual ligands that gave good scores with the three studied targets and can be used as a model to design new dual inhibitors are ligand number 19 for AChE and BuChE duality and ligand number 15 for the BuChE and Aβ duality.

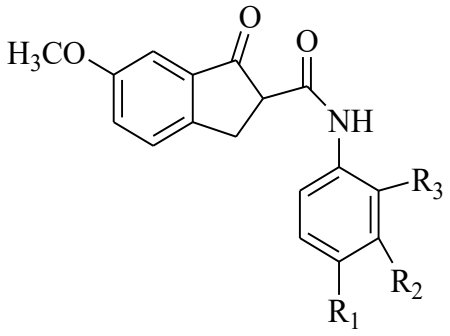

Lig	R_1	R_2	R_3
Lig1	H	H	H
Lig2	CH_3	H	H
Lig3	C_2H_5	H	H
Lig4	OCH_3	H	H
Lig5	OC_2H_5	H	H
Lig6	F	H	H
Lig7	Cl	H	H
Lig8	Br	H	H
Lig9	H	CH_3	H
Lig10	H	C_2H_5	H
Lig11	H	OCH_3	H
Lig12	H	OC_2H_5	H
Lig13	H	F	H
Lig14	H	Cl	H
Lig15	H	Br	H
Lig16	H	H	CH_3
Lig17	H	H	C_2H_5
Lig18	H	H	OCH_3
Lig19	H	H	OC_2H_5
Lig20	H	H	F
Lig21	H	H	CL
Lig22	H	H	Br

Figure 1. The Molecular Structures Corresponding to the 22 Ligands

Table 1. Molecules Names and IC_{50} against AChE, BthE, and Aβ and obtained Ligands Properties using MOE of Compounds (**1**-**22**)

Compounds	IUPAC name	Molecular Formula	AChE IC_{50} (µM)	BthE IC_{50} (µM)	Aβ IC_{50}(µM)	Weight (g/mol)	TPSA (A^2)	LogP	LogS	Toxicity
1	2,3-dihydro-6-methoxy-1-oxo-*N*-phenyl-1*H*-indene-2-carboxamide	$C_{17}H_{15}O_3N$	0.92	3.15	14.3	311.34	64.63	2.70	-3.73	non
2	2,3-dihydro-6-methoxy-1-oxo-*N*-*p*-tolyl-1*H*-indene-2-carboxamide	$C_{18}H_{17}O_3N$	0.84	2.5	26.8	325.36	64.63	3.01	-4.20	non
3	*N*-(4-ethylphenyl)-2,3-dihydro-6-methoxy-1-oxo-1*H*-indene-2-carboxamide	$C_{19}H_{19}O_3N$	0.65	2.96	32.1	339.39	64.63	3.26	-4.72	non

4	2,3-dihydro-6-methoxy-*N*-(4-methoxyphenyl)-1-oxo-1*H*-indene-2-carboxamide	$C_{18}H_{15}O_4N$	0.53	2.9	34.5	341.36	73.86	2.71	-3.78	non
5	*N*-(4-ethoxyphenyl)-2,3-dihydro-6-methoxy-1-oxo-1*H*-indene-2-carboxamide	$C_{19}H_{19}O_4N$	0,58	2,61	40,8	355.39	73.86	3.10	-4.10	non
6	*N*-(4-fluorophenyl)-2,3-dihydro-6-methoxy-1-oxo-1*H*-indene-2-carboxamide	$C_{17}H_{14}O_3NF$	0.11	2.65	45.4	329.33	64.63	2.84	-4.02	non
7	*N*-(4-chlorophenyl)-2,3-dihydro-6-methoxy-1-oxo-1*H*-indene-2-carboxamide	$C_{17}H_{14}O_3NCl$	0.5	4.4	38.2	345.78	64.63	3.35	-4.46	non
8	*N*-(4-bromophenyl)-2,3-dihydro-6-methoxy-1-oxo-1*H*-indene-2-carboxamide	$C_{17}H_{14}O_3NBr$	0.14	3.66	47.6	390.23	64.63	3.46	-4.82	non
9	2,3-dihydro-6-methoxy-1-oxo-*N*-*m*-tolyl-1*H*-indene-2-carboxamide	$C_{18}H_{17}O_3N$	0.77	2.24	19.1	325.36	64.63	3.01	-4.20	non
10	*N*-(3-ethylphenyl)-2,3-dihydro-6-methoxy-1-oxo-1*H*-indene-2-carboxamide	$C_{19}H_{19}O_3N$	0.67	2.98	27.4	339.39	64.63	3.26	-4.72	non
11	2,3-dihydro-6-methoxy-*N*-(3-methoxyphenyl)-1-oxo-1*H*-indene-2-carboxamide	$C_{18}H_{15}O_4N$	0.54	2.1	30.2	341.36	73.86	2.71	-3.78	non
12	*N*-(3-ethoxyphenyl)-2,3-dihydro-6-methoxy-1-oxo-1*H*-indene-2-carboxamide	$C_{19}H_{19}O_4N$	0.78	3.87	28.3	355.39	73.86	3.10	-4.10	non
13	*N*-(3-fluorophenyl)-2,3-dihydro-6-methoxy-1-oxo-1*H*-indene-2-carboxamide	$C_{17}H_{14}O_3NF$	0,247	2,25	38,7	329.33	64.63	2.84	-4.02	non
14	*N*-(3-chlorophenyl)-2,3-dihydro-6-methoxy-1-oxo-1*H*-indene-2-carboxamide	$C_{17}H_{14}O_3NCl$	0.47	2.24	37.4	345.78	64.63	3.35	-4.46	non

15	*N*-(3-bromophenyl)-2,3-dihydro-6-methoxy-1-oxo-1*H*-indene-2-carboxamide	$C_{17}H_{14}O_3NBr$	0.33	2.43	31.9	390.23	64.63	3.46	-4.82	non
16	2,3-dihydro-6-methoxy-1-oxo-*N*-*o*-tolyl-1*H*-indene-2-carboxamide	$C_{19}H_{19}O_3N$	0.36	3.06	40.3	325.36	64.63	3.01	-3.89	non
17	*N*-(2-ethylphenyl)-2,3-dihydro-6-methoxy-1-oxo-1*H*-indene-2-carboxamide	$C_{19}H_{19}O_3N$	0,86	6,29	21,8	339.39	64.63	3.26	-4.40	non
18	2,3-dihydro-6-methoxy-*N*-(2-methoxyphenyl)-1-oxo-1*H*-indene-2-carboxamide	$C_{18}H_{15}O_4N$	0.7	4.81	25.6	341.36	73.86	2.71	-3.78	non
19	*N*-(2-ethoxyphenyl)-2,3-dihydro-6-methoxy-1-oxo-1*H*-indene-2-carboxamide	$C_{19}H_{19}O_4N$	0.77	6.62	38.1	355.39	73.86	3.10	-4.10	non
20	*N*-(2-fluorophenyl)-2,3-dihydro-6-methoxy-1-oxo-1*H*-indene-2-carboxamide	$C_{17}H_{14}O_3NF$	0.08	3.21	55.3	329.33	64.63	2.84	-4.02	non
21	*N*-(2-chlorophenyl)-2,3-dihydro-6-methoxy-1-oxo-1*H*-indene-2-carboxamide	$C_{17}H_{14}O_3NCl$	0.3	7.1	40.4	345.78	64.63	3.35	-4.46	non
22	*N*-(2-bromophenyl)-2,3-dihydro-6-methoxy-1-oxo-1*H*-indene-2-carboxamide	$C_{17}H_{14}O_3NBr$	0.12	3.4	52.8	390.23	64.63	3.46	-4.82	non

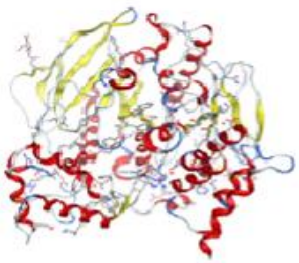

a)

b)

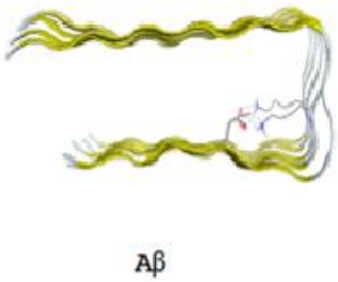

c)

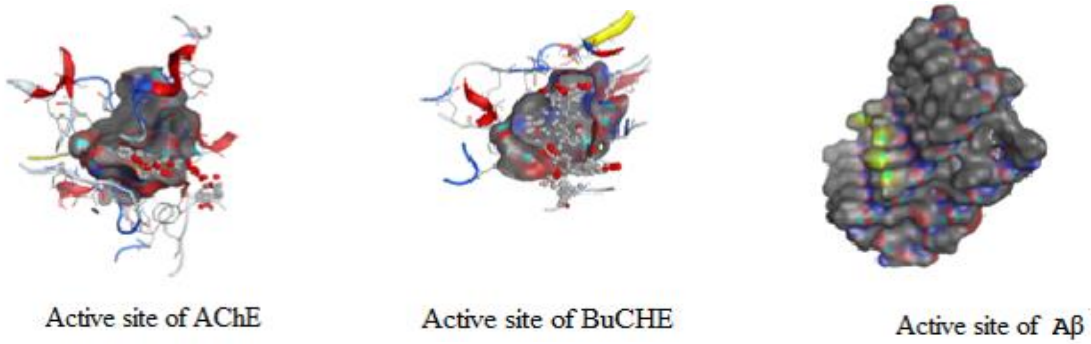

d) e) f)

Figure 2. Downloaded Native Structures of the Enzymes and the Isolated Active Sites

Table 2. Statistical Quality of QSAR Models Developed based on Different Division Tools for AChE, BuChE and Aβ

Validation	Metrics	Model 1	Model 2	Model 3	Model 4	Threshold
Internal AChE	N Training	17	17	17	17	
	N Test	5	5	5	5	
	R^2	0,83223	0,88363	0,87785	0,84621	> 0.5
	RMSE	0.16298	0,13076	0,18035	0,28021	
	R^2cv	0.68580	0.58241	0.679664	0.66739	> 0.5
	$Z-SCORE	1.9482 < ZS < 1.3056	0.6946 < ZS < 1.142	0.7767 < ZS < 1.0272	0.5046 < ZS < 2.0840	< 2.5
External			$R^2_{test\ 0.9606}$			
	RMSE test		0.9801			
Model Equation		Ache pic50 = 1.17613 -0.14325 * chi0v_C +0.06162 * PEOE_VSA_POL -0.16995 * vsurf_Wp4	Ache pic50 = -1.18719 -0.15561 * E_str +0.29230 * PM3_IP -0.17014 * PM3_LUMO +0.09599 * SMR_VSA2 +0.04150 * SMR_VSA3 -0.13785 * vsurf_Wp4	Ache pic50 = 1.56209 -0.13651 * E_str -0.17214 * PM3_LUMO +0.10080 * SMR_VSA2 +0.02918 * SMR_VSA3 -0.13451 * vsurf_Wp4	Ache pic50 = -2.80053 +0.17094 * MNDO_dipole +0.01555 * PEOE_VSA+0 +0.06022 * PEOE_VSA_HYD +0.12946 * PEOE_VSA_POL -0.02129 * PEOE_VSA_POS -0.03965 * vdw_vol	
			BuChE			
Validation	Metrics	Model 5	Model 6	Model 7	Model 8	Threshold
Internal	N Training	17	17	17	17	
	N Test	5	5	5	5	
	R^2	0,69735	0,74745	0,70206	.71239	> 0.5
	RMSE	0,09627	0,09220	0,09981	0,09170	
	R^2cv	0.51263	0.55450	0.51057	0.53343	> 0.5
	$Z-SCORE	0.4548<ZS<0.6322	0.7161<ZS<0.5254	0.4136<ZS<0.1081	0.5859<ZS<0.9151	< 2.5
External			$R^2_{test0.9566}$			
	RMSE test		0.9781			

Model Equation		Bthe pic50 = -1.95177 -0.02273 * MNDO_dipole -0.04080 * vsurf_DD12 -0.01469 * vsurf_HB3 +0.15864 * vsurf_ID3 +0.15076 * vsurf_ID4 +0.01556 * vsurf_W3	Bthe pic50 = -0.86927 -0.03012 * E_oop -0.02579 * MNDO_dipole -0.04784 * vsurf_DD12 +0.00154 * vsurf_HB3 +0.42363 * vsurf_ID3 -0.25670 * vsurf_ID4	Bthe pic50 = -1.15305 -0.01916 * E_ele +0.00508 * MNDO_dipole -0.04552 * vsurf_DD12 +0.00060 * vsurf_HB3 +0.06793 * vsurf_ID3 +0.07737 * vsurf_ID4	Bthe pic50 = -0.97705 -1.79169 * npr1 +1.09797 * vsurf_CP +1.14182 * vsurf_CW4 -0.70721 * vsurf_Wp6

Aβ						
Validation	Metrics	Model 9	Model 10	Model 11	Model 12	Threshold
Internal	N Training	17	17	17	17	
	N Test	5	5	5	5	
	R^2	0,75408	0,75952	0,76745	0,74128	>0.5
	RMSE	0,11735	0,11516	0,11840	0,11386	
	R^2cv	0.49967	0.51508	0.52146	0.52535	
	$Z-SCORE	2.10945<ZS<0.3466	2.0979<ZS<0.5309	1.3243<ZS<0.2875	2.3291<ZS<0.4602	<2.5
External		$R^2_{test\ 0.9011}$				
	RMSE test				0.9492	
Model Equation		Aβpic50 = -1.42650 -1.98824 * a_ICM +1.88270 * density +11.32901 * vsurf_HL1 +0.25480 * vsurf_ID1 +0.11959 * vsurf_ID6	Aβpic50 = -1.42270 -2.13016 * a_ICM +2.18384 * density +11.71892 * vsurf_HL1 +0.68498 * vsurf_ID1 -0.30229 * vsurf_ID2	Aβpic50 = -2.00729 -2.13629 * a_ICM +2.50472 * density +11.00672 * vsurf_HL1 +0.41933 * vsurf_ID1 +0.24070 * vsurf_ID8	Aβpic50 = -1.49915 -2.08249 * a_ICM +2.18037 * density +11.48446 * vsurf_HL1 +0.40971 * vsurf_ID1	

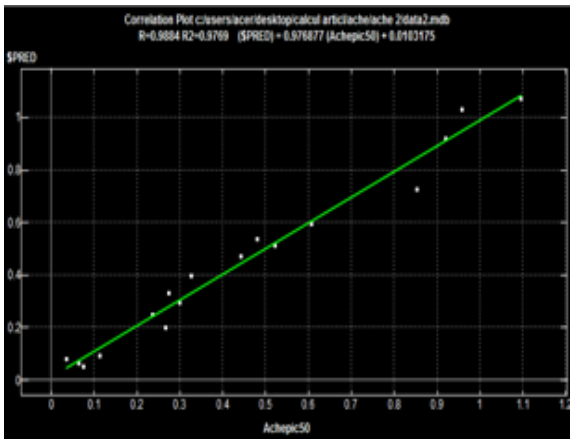

a) Model 2 (AChE)

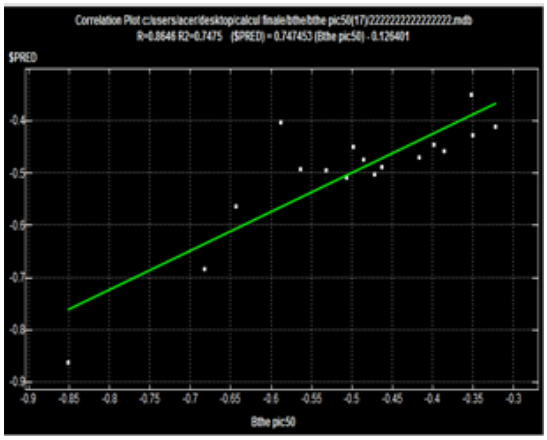

b) Model 6 (BuChE)

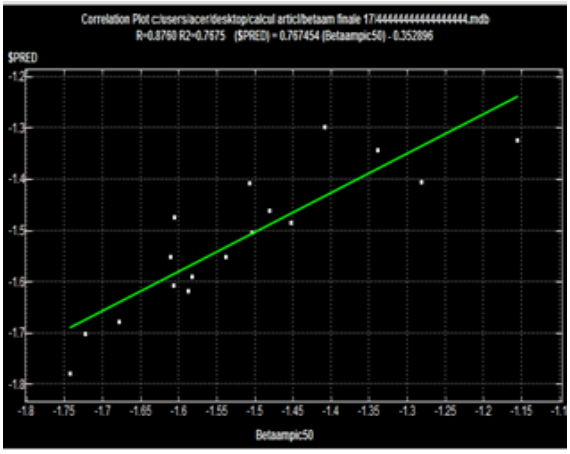

c) Model 11(Aβ)

Figure 3. Correlation Plots between Predicted and Experimental Activities Expressed $pIC_{50}$for AChE, BuChE and Aβ

Ligands Interactions Maps between the Best Ligands Scored Ligands and BuChE

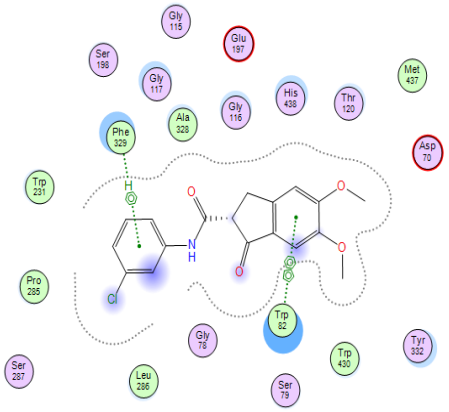

1Lig(14)

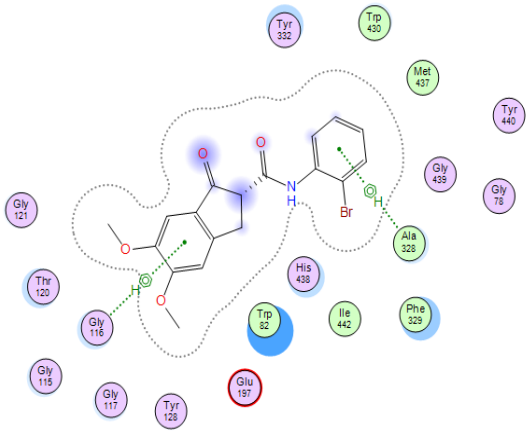

2Lig(22)

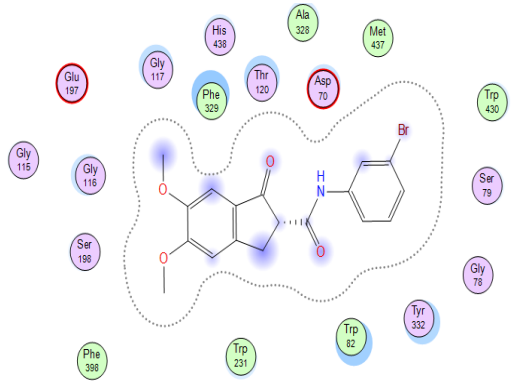

3Lig(15)

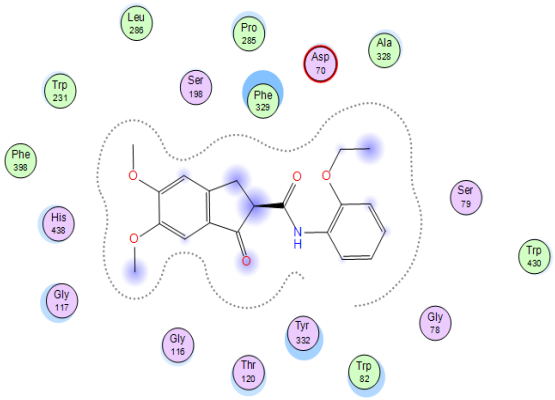

4 Lig(19)

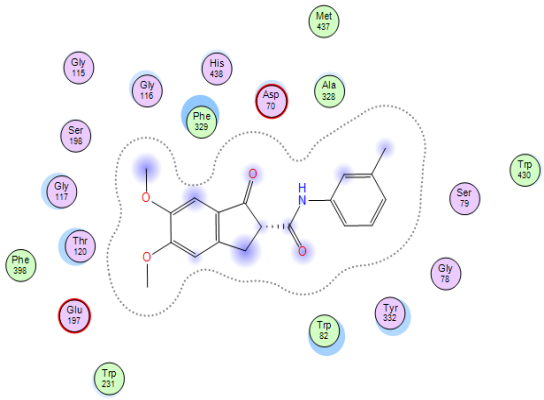

5Lig(9)

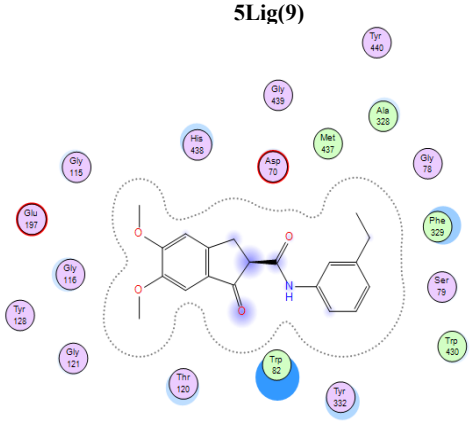

6Lig(10)

Ligands Interactions Maps between the Best Ligands

Scored Ligands and Aβ

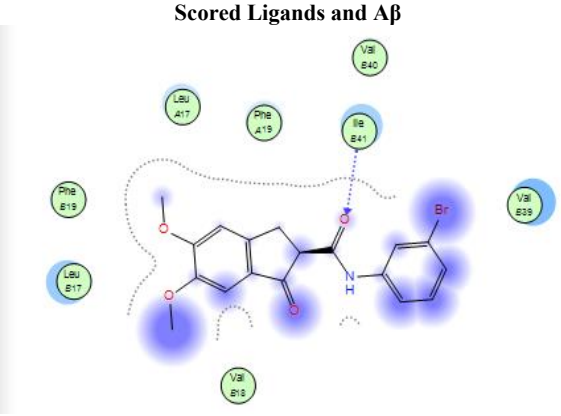

1 lig(15)

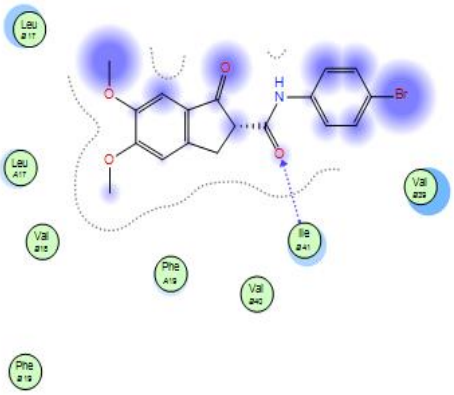

2 lig(8)

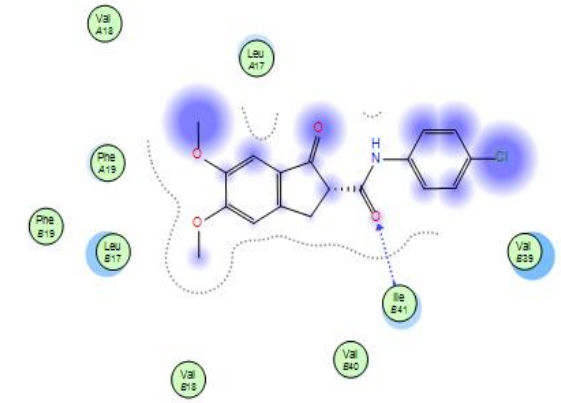

3 lig(7)

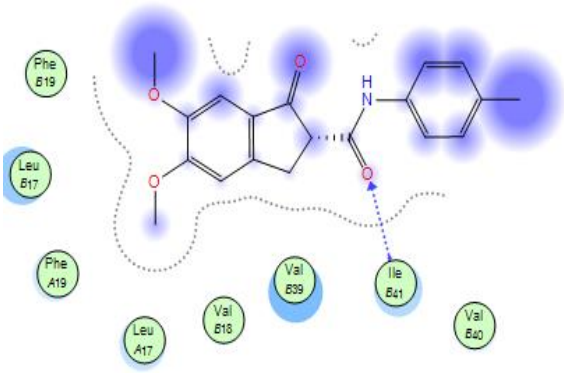

4 lig(2)

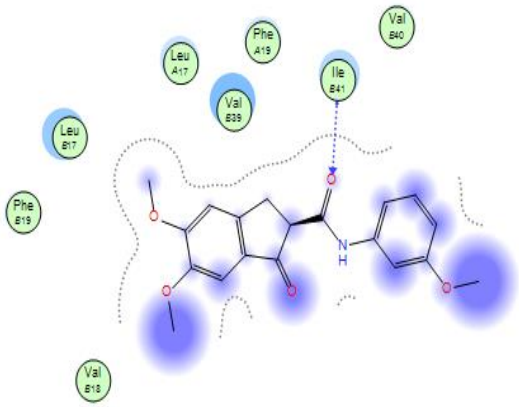

5 lig(11)

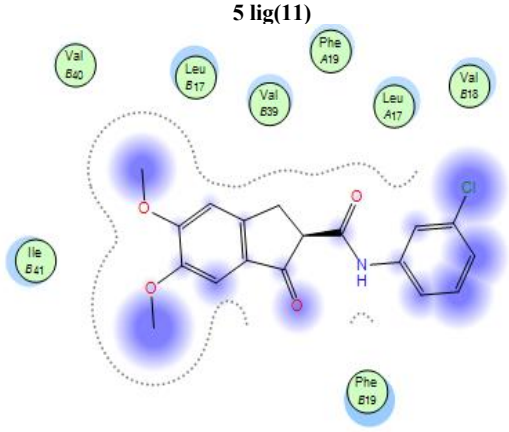

6 lig(14)

Figure 4. Ligands Interactions Maps between the Best Ligands Scored Ligands and Enzymes

AChE

a)

BuChE

b)

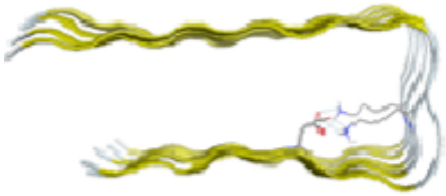

Aβ

c)

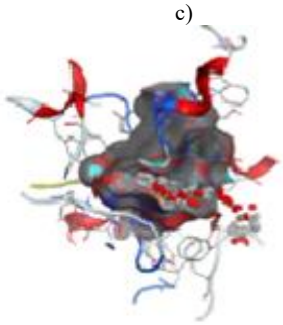

Active site of AChE

d)

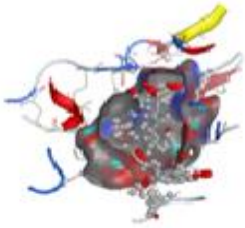

Active site of BuCHE

e)

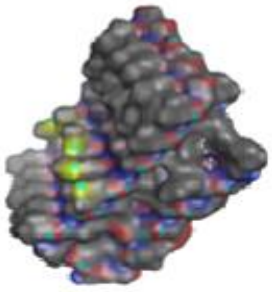

Active site of Aβ

f)

Figure 5. Downloaded Native Structures of the Enzymes and the Isolated Active Sites

Conclusion

To develop anti-Alzheimer's therapies, the amyloid-β and cholinergic pathways that lead to amyloid plaques are the main targets. The inhibitory activity and structure of a series of dual inhibitors of certain targets involved in these pathways are discussed in this work. Our results indicated that for the design of new dual drugs for Alzheimer's disease one can take the donepezil derivatives as a basic structure, the combinations of the three structures found in our study as the best scored (AChE (-8.1299 kcal/mol, ligand 4), BuChE (-7.0399 kcal/mol, ligand 14) and Aβ (-4.8651 kcal/mol, ligand 15), can lead us to the development of the new drug, on the other hand, the elaborated QSAR models for the three studied enzymes gave us an idea about what descriptors are the best for getting better ligands. The important descriptors are linked with the ionization potential and the surface and volume of the ligands. Our findings confirmed that the various computational tools combination gives supplementary information on the kind of interactions between enzyme ligands complex formation and ligands and active site residues, which is impossible experimentally.

Acknowledgments: Authors are thankful to the Directorate-General for Scientific Research and Technological Development (DGRSDT) under the authority of the Algerian Ministry of Higher Education and Scientific Research for supporting this work as part of the PRFU project number B00L01EP130220190002.

Conflict of interest: None

Financial support: None

Ethics statement: None

References

Aranda-Abreu, G. E., Hernández-Aguilar, M. E., Denes, J. M., Hernández, L. I. G., & Rivero, M. H. (2011). Rehabilitating a brain with Alzheimer's: a proposal. *Clinical Interventions in Aging*, *6*, 53-59.

Bamidis, P. D., Tarnanas, I., Hadjileontiadis, L., & Tsolaki, M. (2020). *Handbook of research on innovations in the diagnosis and treatment of dementia*. Advances in psychology, mental health, and behavioral studies (APMHBS) book series. xxvii, 511 p.

Banner, C. D. B., & Nixon, R. A. (1992). *Proteases and protease inhibitors in Alzheimer's disease pathogenesis*. Annals of the New York Academy of Sciences. New York, N.Y.: New York Academy of Sciences. x, 259 p.

Chemical Computing Group Inc. (2016). Molecular operating environment (MOE). *Chemical Computing Group Inc 1010 Sherbooke St. West, Suite# 910, Montreal.*

Daramola, D. A., Muthuvel, M., & Botte, G. G. (2010). Density functional theory analysis of Raman frequency modes of monoclinic zirconium oxide using Gaussian basis sets and

isotopic substitution. *The Journal of Physical Chemistry B*, *114*(29), 9323-9329.

Engh, R. A., & Huber, R. (1991). Accurate bond and angle parameters for X-ray protein structure refinement. *Acta Crystallographica Section A: Foundations of Crystallography*, *47*(4), 392-400.

Golbraikh, A., Shen, M., Xiao, Z., Xiao, Y. D., Lee, K. H., & Tropsha, A. (2003). Rational selection of training and test sets for the development of validated QSAR models. *Journal of computer-aided molecular design*, *17*(2), 241-253.

Gu, X., Wang, Y., Wang, M., Wang, J., & Li, N. (2021). Computational investigation of imidazopyridine analogs as protein kinase B (Akt1) allosteric inhibitors by using 3D-QSAR, molecular docking and molecular dynamics simulations. *Journal of Biomolecular Structure and Dynamics*, *39*(1), 63-78.

Hardiman, O., Doherty, C. P., Elamin, M., & Bede, P. (2016). *Neurodegenerative Disorders: A Clinical Guide*. p. 1 online resource (X, 336 pages 49 illustrations, 19 illustrations in color.).

Harris, R. E. (2019). *Epidemiology of chronic disease: global perspectives*. Jones & Bartlett Learning.

Hiscocks, J., & Frisch, M. J. (2009). *Gaussian 09: IOps Reference*. M. Caricato, & M. J. Frisch (Eds.). Gaussian.

Höltje, H. D. (2008). *Molecular modeling: basic principles and applications*. 3rd, rev. and expanded ed., Weinheim: Wiley-VCH.

Jalali-Heravi, M., & Kyani, A. (2004). Use of computer-assisted methods for the modeling of the retention time of a variety of volatile organic compounds: a PCA-MLR-ANN approach. *Journal of chemical information and computer sciences*, *44*(4), 1328-1335.

Kapetanovic, I. M. (2008). Computer-aided drug discovery and development (CADDD): in silico-chemico-biological approach. *Chemico-biological interactions*, *171*(2), 165-176.

Kasmi, R., Hadaji, E., Chedadi, O., El Aissouq, A., Bouachrine, M., & Ouammou, A. (2020). 2D-QSAR and docking study of a series of coumarin derivatives as inhibitors of CDK (anticancer activity) with an application of the molecular docking method. *Heliyon*, *6*(8), e04514.

Khosravan, A., Marani, S., & Googheri, M. S. S. (2017). The effects of fluorine substitution on the chemical properties and inhibitory capacity of Donepezil anti-Alzheimer drug; density functional theory and molecular docking calculations. *Journal of Molecular Graphics and Modelling*, *71*, 124-134.

Kovačević, S., Karadžić, M., Podunavac-Kuzmanović, S., & Jevrić, L. (2018). Binding affinity toward human prion protein of some anti-prion compounds—Assessment based on QSAR modeling, molecular docking and non-parametric ranking. *European Journal of Pharmaceutical Sciences*, *111*, 215-225.

Kukol, A. (Ed.). (2008). *Molecular modeling of proteins* (Vol. 443). Totowa, NJ: Humana Press.

Kuncharoenwirat, N., Chatuphonprasert, W., & Jarukamjorn, K. (2020). Effects of Phenol Red On Rifampicin-Induced Expression of Cytochrome P450s Enzymes. *Pharmacophore, 11*(3), 13-20.

Lajtha, A., & Banik, N. L. (2001). *Role of proteases in the pathophysiology of neurodegenerative diseases*. New York: Kluwer Academic/Plenum Publishers. xii, 302 p.

Lee, V. M. Y. (2000). *Fatal attractions: protein aggregates in neurodegenerative disorders*. Research and perspectives in Alzheimer's disease. Berlin; New York: Springer. xii, 140 p.

Li, K., Zhu, J., Xu, L., & Jin, J. (2019). Rational Design of Novel Phosphoinositide 3-Kinase Gamma (PI3Kγ) Selective Inhibitors: A Computational Investigation Integrating 3D-QSAR, Molecular Docking and Molecular Dynamics Simulation. *Chemistry & Biodiversity*, *16*(7), e1900105.

Lilford, P., & Hughes, J. C. (2020). Epidemiology and mental illness in old age. *BJPsych Advances*, *26*(2), 92-103.

Mahmud, A. W., Shallangwa, G. A., & Uzairu, A. (2020). QSAR and molecular docking studies of 1, 3-dioxoisoindoline-4-aminoquinolines as potent antiplasmodium hybrid compounds. *Heliyon*, *6*(3), e03449.

Piguet, P., & Poindron, P. (2012). *Genetically modified organisms and genetic engineering in research and therapy*. BioValley monographs. Basel; New York: Karger. xiv, 123 p.

Ronson, C. E. (2011). *Alzheimer's Diagnosis*. Nova Science Publishers.

Roy, A., Rasheed, A., Sleeba, A. V., & Rajagopal, P. (2020). Molecular docking analysis of capsaicin with apoptotic proteins. *Bioinformation*, *16*(7), 555-560.

Royal Society of Chemistry (Great Britain). (2014). Faraday Division, *Molecular simulations, and visualization: University of Nottingham, Nottingham UK*. Faraday discussions. 535 pages.

Sargazi, M., & Taghian, F. (2020). The Effect of Royal Jelly and Exercise on Liver Enzymes in Addicts. *Archives of Pharmacy Practice*, *11*(2), 96-101.

Shamsi, A., Al Shahwan, M., Ahamad, S., Hassan, M. I., Ahmad, F., & Islam, A. (2020). Spectroscopic, calorimetric and molecular docking insight into the interaction of Alzheimer's drug donepezil with human transferrin: Implications of Alzheimer's drug. *Journal of Biomolecular Structure and Dynamics*, *38*(4), 1094-1102.

Sigurdsson, E. M., Calero, M., & Gasset, M. (2012). *Amyloid proteins: methods and protocols*. 2nd ed. Methods in molecular biology. 2012, New York: Humana Press. xv, 548 p.

Stonebrook, M. J. (2007). *Creutzfeldt-Jakob disease: new research*. New York: Nova Biomedical Books. xi, 159 p.

Taha, M. O., & AlDamen, M. A. (2005). Effects of variable docking conditions and scoring functions on corresponding protein-aligned comparative molecular field analysis models constructed from diverse human protein tyrosine phosphatase 1B inhibitors. *Journal of medicinal chemistry*, *48*(25), 8016-8034.

Tappen, R. M. (1997). *Interventions for Alzheimer's disease: A caregiver's complete reference*. Health Professions Press.

Uddin, M., & Amran, M. (Eds.). (2018). *Handbook of research on critical examinations of neurodegenerative disorders*. IGI Global.

Vicente, J. M. F., Álvarez-Sánchez, J. R., De la Paz López, F., Toledo-Moreo, F. J., & Adeli, H. (Eds.). (2015). Artificial computation in biology and medicine: international work-conference on the interplay between natural and artificial computation, IWINAC 2015*, Elche, Spain, June 1-5, 2015, Proceedings, Part I* (Vol. 9107). Springer.

Wallin, Å. K., Andreasen, N., Eriksson, S., Båtsman, S., Näsman, B., Ekdahl, A., Kilander, L., Grut, M., Rydén, M., Wallin, A., et al. (2007). Donepezil in Alzheimer's disease: what to expect after 3 years of treatment in a routine clinical setting. *Dementia and Geriatric Cognitive Disorders*, *23*(3), 150-160.

Wehrens, R., & Mevik, B. H. (2007). The pls package: principal component and partial least squares regression in R. *Journal of Statistical Software, 18*(2), 1-23.

Yerdelen, K. O., Koca, M., Anil, B., Sevindik, H., Kasap, Z., Halici, Z., Turkaydin, K., & Gunesacar, G. (2015). Synthesis of donepezil-based multifunctional agents for the treatment of Alzheimer's disease. *Bioorganic & Medicinal Chemistry Letters*, *25*(23), 5576-5582.